



Simulation of massless Dirac dynamics in plasmonic waveguide arrays

BEIBEI XU, TAO LI,* AND SHINING ZHU

National Laboratory of Solid State Microstructures, College of Engineering and Applied Sciences,
Collaborative Innovation Center of Advanced Microstructures, Nanjing University, Nanjing 210093,
China

*taoli@nju.edu.cn

Abstract: The recent simulation of quantum behavior in condensed matter physics by well-designed photonic structures has opened unprecedented opportunities to steer the flow of light in novel manners. Here, we propose a design to simulate massless Dirac dynamics in evanescently coupled plasmonic ridge waveguide arrays with alternating positive and negative coupling coefficients. The coupling coefficients are carefully tailored by adjusting the geometric parameters of the waveguide in arrays, which are supposed to be feasible with advanced nanofabrication techniques. Further theoretical studies are also carried out based on the coupled mode theory to discuss the influence of excitation condition on beam propagation in this massless Dirac dynamics simulation case.

© 2018 Optical Society of America under the terms of the [OSA Open Access Publishing Agreement](#)

OCIS codes: (240.6680) Surface plasmons; (230.7370) Waveguides; (260.2030) Dispersion.

References and links

1. S. Longhi, "Quantum-optical analogies using photonic structures," *Laser Photonics Rev.* **3**(3), 243–261 (2009).
2. S. Longhi, "Classical simulations of relativistic quantum mechanics in periodic optical structures," *Appl. Phys. B* **104**(3), 453–468 (2011).
3. A. Trabesinger, "Quantum simulation," *Nat. Phys.* **8**(4), 263 (2012).
4. D. N. Christodoulides, F. Lederer, and Y. Silberberg, "Discretizing light behaviour in linear and nonlinear waveguide lattices," *Nature* **424**(6950), 817–823 (2003).
5. F. Lederer, G. I. Stegeman, D. N. Christodoulides, M. Segev, G. Assanto, and Y. Silberberg, "Discrete solitons in optics," *Phys. Rep.* **463**(1-3), 1–126 (2008).
6. H. S. Eisenberg, Y. Silberberg, R. Morandotti, and J. S. Aitchison, "Diffraction Management," *Phys. Rev. Lett.* **85**(9), 1863–1866 (2000).
7. T. Pertsch, P. Dannberg, W. Elflein, A. Brauer, and F. Lederer, "Optical Bloch oscillations in temperature tuned waveguide arrays," *Phys. Rev. Lett.* **83**(23), 4752–4755 (1999).
8. A. Block, C. Etrich, T. Limboeck, F. Bleckmann, E. Soergel, C. Rockstuhl, and S. Linden, "Bloch oscillations in plasmonic waveguide arrays," *Nat. Commun.* **5**, 3843 (2014).
9. W. Zhang and S. E. Ulloa, "ac-field-controlled localization-delocalization transition in a one-dimensional disordered system," *Phys. Rev. B* **74**(11), 115304 (2006).
10. Y. Lahini, A. Avidan, F. Pozzi, M. Sorel, R. Morandotti, D. N. Christodoulides, and Y. Silberberg, "Anderson Localization and Nonlinearity in One-Dimensional Disordered Photonic Lattices," *Phys. Rev. Lett.* **100**(1), 013906 (2008).
11. S. Longhi, M. Marangoni, M. Lobino, R. Ramponi, P. Laporta, E. Cianci, and V. Foglietti, "Observation of Dynamic Localization in Periodically Curved Waveguide Arrays," *Phys. Rev. Lett.* **96**(24), 243901 (2006).
12. A. Szameit, I. L. Garanovich, M. Heinrich, A. A. Sukhorukov, F. Dreisow, T. Pertsch, S. Nolte, A. Tünnermann, and Y. S. Kivshar, "Polychromatic dynamic localization in curved photonic lattices," *Nat. Phys.* **5**(4), 271–275 (2009).
13. R. Gerritsma, G. Kirchmair, F. Zähringer, E. Solano, R. Blatt, and C. F. Roos, "Quantum simulation of the Dirac equation," *Nature* **463**(7277), 68–71 (2010).
14. S. H. Nam, A. J. Taylor, and A. Efimov, "Diabolical point and conical-like diffraction in periodic plasmonic nanostructures," *Opt. Express* **18**(10), 10120–10126 (2010).
15. S. Longhi, "Klein tunneling in binary photonic superlattices," *Phys. Rev. B* **81**(7), 075102 (2010).
16. F. Dreisow, M. Heinrich, R. Keil, A. Tünnermann, S. Nolte, S. Longhi, and A. Szameit, "Classical Simulation of Relativistic Zitterbewegung in Photonic Lattices," *Phys. Rev. Lett.* **105**(14), 143902 (2010).
17. S. L. Ding and G. P. Wang, "Plasmonic analogs of Zitterbewegung in nanoscale metal waveguide arrays," *J. Opt. Soc. Am. B* **31**(3), 603 (2014).
18. S. H. Nam, J. Zhou, A. J. Taylor, and A. Efimov, "Dirac dynamics in one-dimensional graphene-like plasmonic crystals: pseudo-spin, chirality, and diffraction anomaly," *Opt. Express* **18**(24), 25329–25338 (2010).

19. S. H. Nam, E. Ulin-Avila, G. Bartal, and X. Zhang, "General properties of surface modes in binary metal-dielectric metamaterials," *Opt. Express* **18**(25), 25627–25632 (2010).
20. J. M. Zeuner, N. K. Efremidis, R. Keil, F. Dreisow, D. N. Christodoulides, A. Tünnermann, S. Nolte, and A. Szameit, "Optical analogues for massless Dirac particles and conical diffraction in one dimension," *Phys. Rev. Lett.* **109**(2), 023602 (2012).
21. Q. Q. Cheng, Y. M. Pan, Q. J. Wang, T. Li, and S. N. Zhu, "Topologically protected interface mode in plasmonic waveguide arrays," *Laser Photonics Rev.* **9**(4), 392–398 (2015).
22. Y. M. Liu and X. Zhang, "Metasurface for manipulating surface plasmons," *Appl. Phys. Lett.* **103**(14), 141101 (2013).
23. A. A. High, R. C. Devlin, A. Dibos, M. Polking, D. S. Wild, J. Perczel, N. P. de Leon, M. D. Lukin, and H. Park, "Visible-frequency hyperbolic metasurface," *Nature* **522**(7555), 192–196 (2015).
24. R. F. Oulton, V. J. Sorger, D. A. Genov, D. F. P. Pile, and X. Zhang, "A hybrid plasmonic waveguide for subwavelength confinement and long-range propagation," *Nat. Photonics* **2**(8), 496–500 (2008).
25. H. B. Perets, Y. Lahini, F. Pozzi, M. Sorel, R. Morandotti, and Y. Silberberg, "Realization of quantum walks with negligible decoherence in waveguide lattices," *Phys. Rev. Lett.* **100**(17), 170506 (2008).
26. A. Peruzzo, M. Lobino, J. C. F. Matthews, N. Matsuda, A. Politi, K. Poullos, X. Q. Zhou, Y. Lahini, N. Ismail, K. Wörhoff, Y. Bromberg, Y. Silberberg, M. G. Thompson, and J. L. O'Brien, "Quantum walks of correlated photons," *Science* **329**(5998), 1500–1503 (2010).
27. P. B. Johnson and R. W. Christy, "Optical Constants of the Noble Metals," *Phys. Rev. B* **6**(12), 4370–4379 (1972).

1. Introduction

Quantum simulation is aimed to use a more controllable system to reproduce the quantum dynamics that is hardly accessible in experiments [1–3]. The research of this quantum-optical analog has been greatly stimulated by the development of discrete optics [4, 5], which is designed to realize novel functionalized optical materials based on evanescently coupled optical waveguides. In coupled waveguide arrays, the dispersion and diffraction properties of light can be particularly managed [6]. The key point that one can map nonrelativistic quantum mechanics onto the waveguide arrays is the similarity between the Schrödinger equation for matter waves and the scalar paraxial wave equation for optical waves [1, 2]. Optical analogues of electronic Bloch oscillations [7, 8], Anderson localization [9, 10] and dynamic localization [11, 12] have been proposed. Recently, the investigation of simulating certain fundamental phenomena rooted in relativistic wave equations, such as Dirac equation for fermionic particles, has held much attention [13–17].

It is well known that the band structure of a massless Dirac equation is characterized by a particular conical intersection point between the two bands which is termed as the Dirac point or diabolic point. This point features its singularity near which the frequency dispersion of the optical modes is linear. Therefore, it gives rise to a peculiar nondispersive conical diffraction. It has been theoretically proposed by a periodic metal-dielectric waveguide array that can form such a singular point in k -space to simulate massless Dirac dynamics [14, 18]. The singularity stems from the balance between alternating positive and negative couplings, which are obtained through dielectric layer and metal layer respectively [19]. However, it was never demonstrated in experiments due to the great difficulty to access such almost infinite multilayers structure. Instead this phenomenon was later realized in a waveguide array that consists of sinusoidally curved waveguides [20]. Nevertheless, the nondispersive conical diffraction is not intuitively shown due to the curved structure. To date, no more direct experimental scheme of the optical analogues for massless Dirac dynamics in waveguide system has been reported.

In this work, we propose a more feasible design with a binary plasmonic ridge waveguide array (PRWA) to simulate the massless Dirac dynamics, in which one-dimensional (1D) nondispersive conical diffractions are verified and demonstrated by full-wave simulations. In the waveguides, the surface plasmon polariton (SPP) modes are of vectorial near-field configurations, which possibly give rise to either positive or negative coupling coefficients when the ridge waveguides are coupled together. In order to simulate the massless Dirac model, we carefully analyzed the mode property of two coupled ridge waveguides and obtained appropriate parameters for positive and negative coupling coefficients. Based on

these parameters, a binary PRWA was designed with alternating gaps between the waveguides, in which a 1D nondispersive conical propagation of SPP wave is well demonstrated by full-wave simulations. Our studies also show such coupling strength can be further modulated or optimized by deforming the shaped of ridge waveguide, and a trapezoid one was proposed to get a better performance. Additionally, the influence of the excitation conditions on the beam evolution was also analyzed in-depth based on coupled mode theory (CMT).

2. Theoretical model and simulation results

2.1 Analogy between massless Dirac dynamics and optical modes in waveguide array

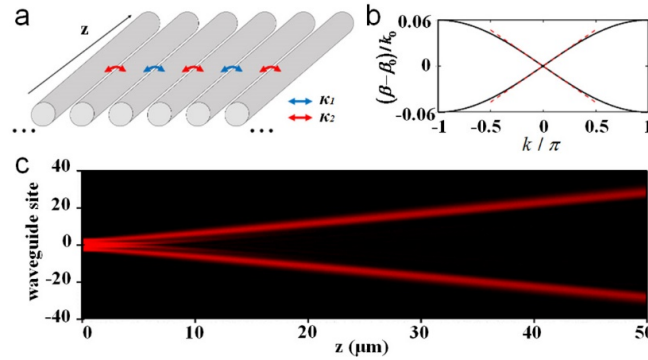


Fig. 1. (a) Schematic of binary waveguide array, where red and blue arrows denote positive and negative coupling coefficients, respectively. (b) Dispersion relation of a binary waveguide array with balanced positive and negative coupling coefficients with the coupling strength is set as $\kappa = 0.03k_0$. (c) CMT calculation results of beam evolution in a binary waveguide array.

Figure 1(a) schematically shows a binary waveguide array with alternating coupling coefficients. The propagation of light in such evanescently coupled waveguides with nearest-neighbor interaction can be described by the tight-binding model as below [14]

$$\begin{cases} \left(i \frac{\partial}{\partial z} + \beta_0 \right) E_{2n} + \kappa_1 E_{2n-1} + \kappa_2 E_{2n+1} = 0 \\ \left(i \frac{\partial}{\partial z} + \beta_0 \right) E_{2n+1} + \kappa_2 E_{2n} + \kappa_1 E_{2n+2} = 0 \end{cases}, \quad (1)$$

where β_0 is the propagation constant of the isolated waveguide, while κ_1 and κ_2 represent the alternating coupling coefficients. The solutions of Eq. (1) are given as $a_n = A \exp(i\beta z + ikn)$ for E_{2n} and $b_n = B \exp(i\beta z + ikn)$ for E_{2n+1} , where k is the transverse wave number multiplied with the array period, A and B are the amplitudes of the eigenmodes a_n and b_n . This coupled mode equations can be transformed into a compact Hamiltonian form as [14, 20]

$$H\psi = (\beta - \beta_0)\psi, \quad (2)$$

$$H = \begin{pmatrix} 0 & \kappa(e^{-ik} - 1) \\ \kappa(e^{ik} - 1) & 0 \end{pmatrix},$$

when the alternating coupling coefficients are opposite numbers, that is $\kappa_1 = -\kappa_2 = \kappa$, and $\psi = (A, B)^T$. This Hamiltonian H for waveguide mode propagating in binary waveguide array shares a familiar form of massless Dirac Hamiltonian for relativistic quantum particles [15]. Thus, the propagation of optical wave in such a binary waveguide array can directly simulate

the temporal evolution of massless Dirac dynamics in its propagation dimension. Solving the Hamiltonian in Eq. (2), we can obtain the dispersive relation of this binary waveguide array with alternating positive and negative coupling coefficients in same amplitude with the dispersion curves of $\beta - \beta_0 = \pm \kappa(2 - 2\cos k)^{1/2}$ as shown in Fig. 1(b), in which the coupling strength $\kappa = 0.03k_0$ ($k_0 = 2\pi/\lambda$ is the wavevector number in free space). It is evident that dispersion curves near the center of Brillouin zone tend to be linear (dashed lines in Fig. 1(b)), which can be easily deduced from the relation of $\beta - \beta_0 = \pm 2\kappa|\sin k/2| \approx \pm \kappa k$ in the range of small k . Hence when one launches a beam with an exact zero transverse k-vector into this waveguide array, the beam will split into two equally nondispersive beams according to the linear dispersion property. To verify it, we performed theoretical calculations on a proper binary waveguides array with two well defined coupling coefficients as $\kappa_1 = 0.03k_0$ and $\kappa_2 = -0.03k_0$ based on coupled mode theory (CMT), as the results shown in Fig. 1(c), which exactly manifests two splitting nondispersive beams agreeing well with the theoretical prediction of one-dimensional (1D) conical diffractions.

2.2 Controlling the coupling coefficients in plasmonic waveguides

According to above analyses, we need to work out a set of balanced positive and negative coupling coefficients in coupled waveguide array to simulate the massless Dirac dynamics [14,20]. Here, we would like to consider the coupled metallic ridge waveguides, which has been demonstrated a wide tunable range in coupling strength and was successfully used to construct a plasmonic topological Su-Schrieffer-Heeger (SSH) array [21]. It was also shown that in a similar plasmonic ridge waveguide array (PRWA) (*i.e.*, a kind of metasurface) diverse dispersions were theoretically demonstrated from positive to negative [22]. In fact, such an interesting dispersion engineering accounts for the adjustable coupling coefficients between the waveguides, though it was explained in a viewpoint of metasurface in Ref [22]. The hyperbolic dispersion was later realized in experiments with PRWA system [23]. Therefore, it is quite reasonable to extend the previous PRWA of SSH model [21] to a balanced positive/negative coupling coefficients. Then, it is ready to analyze the detailed coupling property of two ridge waveguides with respect to the structural parameters.

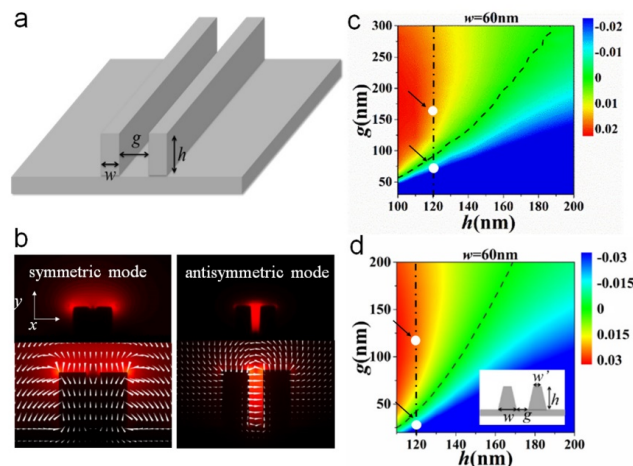


Fig. 2. (a) Schematic diagram of two closely placed rectangle ridge waveguides. (b) Electric field intensity distributions of symmetric mode and antisymmetric mode ($w = 60$ nm and $h = 120$ nm and $g = 30$ nm) and their corresponding vectorial field distributions. (c) Phase graph of coupling coefficients respect to structure parameters g and h for two coupled rectangle ridge waveguides shown as (a) with $w = 60$ nm and (d) for two coupled trapezoid ridge waveguides with $w = 60$ nm and $w' = 20$ nm shown as the inset. The dashed line notes the zero coupling coefficient and the two white points on the dot-dashed line represent the selected parameters in the following simulation.

Employing a commercial finite-element analysis software (Comsol Multiphysics 5.2a), we first calculate the mode property of a single silver ridge waveguide with ridge width of 60 nm ($w = 60$ nm) and height of 120 nm ($h = 120$ nm) at the wavelength $\lambda = 633$ nm and its normalized propagation constant β_0 ($k_{z,\text{spp}}/k_0$) is 1.0679. Note that we ignore the loss (it will be discussed in Section 3.2) for simplification, and as a result the propagation constant keeps a real number. Next, we analyze the coupled case with two closely placed ridge waveguides as schematically shown in Fig. 2(a). As expected there are two eigenmodes obtained due to the coupling effect as symmetric and antisymmetric modes shown as Fig. 2(b), which gives rise to two propagation constants as β_s and β_a , respectively. According to the coupled mode theory, the coupling coefficient can be calculated as $\kappa = (\beta_s - \beta_a)/2$ [24]. Then, we can work out a diagram of the coupling coefficients with respect to the gap (g) and height (h) of two coupled waveguides after a systematic calculation, as the results shown in Fig. 2(c).

By systematic simulations, the phase diagram of the coupling coefficients (from -0.24 to 0.022) for two coupled plasmonic ridge waveguides (PRWs) is plotted in Fig. 2(c) with respect to structure parameters g and h shown in Fig. 2(a), in which a dashed line shows the division boundary between the negative (blue) and positive (red) coupling zones. From Fig. 2(c) we can also find that when the height of waveguides (h) increases, it favors the negative coupling, while increasing the gap (g) favors the positive one. The fact lies in the vectorial configuration of the coupled waveguides, as shown in Fig. 2(b), that the y component of electric field (E_y) inside (and around) the gap would mainly contribute to the positive coupling, and the x component (E_x) to the negative one, according to the field superposition property in a mirror symmetry. Therefore, the geometric parameters greatly affect the strength contrast between the two electric components and will probably change the sign of the coupling coefficients. According to this fact, the shape design of the ridge waveguides can be further optimized to increase the coupling strength (κ) both for the positive and negative coupling ranges. Figure 2(d) shows a new phase diagram of the coupling coefficients based on the waveguides with a trapezoidal cross section, where the maximum of coupling strength is raised to 0.032. It accounts for that the sloping side of the trapezoidal waveguide can contribute more E_y components and will be easier to balance the positive and negative coupling with enhanced intensity. Moreover, such trapezoidal waveguides would be more convenient to access in nanofabrication. In the next section, the enhanced coupling strength will be verified by numerical calculation on the SPP propagation within the waveguide array.

2.3 Simulation of massless Dirac dynamics in plasmonic waveguide array

According the obtained phase diagram in Fig. 2(c), we can appropriately select two sets of parameters for a balanced positive and negative couplings as $g = 160$ nm and 70 nm, with fixed $w = 60$ nm and $h = 120$ nm for $\kappa_1 = 0.0161$ and $\kappa_2 = -0.0162$ respectively (see two white points in the dashed-dot line in Fig. 2(c)). Then, a binary waveguide array is constructed for the COMSOL simulations on the SPP propagations, as shown in Fig. 3(a). Note that we here only change the gap distance with fixed height for the convenience in potential fabrications. In our theoretical modeling, 79 waveguides are designed, inside which a proper illumination condition was defined with 7 waveguides excited (it will be discussed in more details later). The excitation field distribution is shown as Fig. 3(b), which is given by COMSOL with boundary mode analysis. It would be possibly excited by launching the SPP mode using a tapered connection of strip waveguide [21] with the ending width of 7 waveguides. Figure 3(c) shows the simulated field distribution of the SPP propagation from the left to right with a distance of $30 \mu\text{m}$, where two apparent splitting beams are formed without spreading. It agrees well with the massless Dirac dynamics behavior. Since the full-wave simulation is quite time consuming, we didn't perform simulations on a larger scale. In order to unveil the 1D nondispersive conical diffraction more clearly, as well as to verify the influence of the coupling strength, trapezoid ridge waveguides array was also modeled and calculated as the same proceeding as the former one. Here, the parameters are determined as $w = 60$ nm, $w' =$

20 nm, $h = 120$ nm, and $g = 27$ nm and 115 nm (referring from Fig. 2(d)), corresponding to a stronger coupling strength as $\kappa_1 = -0.0254$ and $\kappa_2 = 0.0255$ respectively. The simulation result is shown in Fig. 3(f) with the excitation condition in Fig. 3(e), where more apparently nondispersive splitting beams are demonstrated with larger splitting angle, which does correspond to the enhanced coupling strength as expected. This simulation vividly reproduces the massless Dirac dynamics as the CMT predicted in Fig. 1(c), and ensures the valid of our design.

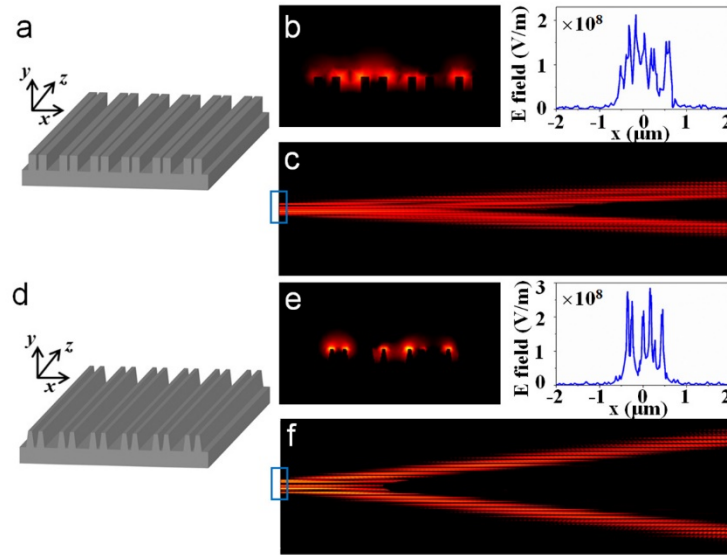


Fig. 3. (a) Schematics of a binary rectangle PRWA with balanced positive and negative coupling by alternating the gaps. (b) Excitation field distributions on 7 waveguides corresponding to the blue box in (c). (c) COMSOL simulation result of the SPP propagation along z-axis in rectangle PRWA of (a). The propagation distance here is 30 μm . (d) Schematics of a binary trapezoid PRWA. (e) Excitation field distributions on 7 waveguides corresponding to the blue box in (f). (f) SPP propagation along z-axis in trapezoid PRWA of (d).

3. Discussions

3.1 Influence of excitation condition

During our simulation process, we find that the 1D nondispersive conical diffraction is much more obvious when we choose seven or more waveguides as the input port. In order to get an insightful understanding of the influence of the excitation condition, we start from the coupled mode equations Eq. (1) for binary waveguide array with alternating positive and negative coupling coefficients as $(\kappa_1, \kappa_2) = (\kappa_+, \kappa_-)$. Because of the similarities between paraxial wave equation and quantum Schrodinger equation, we solve Eq. (1) in a typical quantum way. First, we get the Hamiltonian of the array of 79 waveguides with only diagonal and sub-diagonal elements under nearest-coupling approximation, which is shown as

$$H = \begin{pmatrix} \ddots & \kappa_+ & & & & & \\ \kappa_+ & \beta_0 & \kappa_- & & & & \\ & \kappa_- & \beta_0 & \kappa_+ & & & \\ & & \kappa_+ & \beta_0 & \kappa_- & & \\ & & & \kappa_- & \beta_0 & \ddots & \\ & & & & & \ddots & \ddots \end{pmatrix}_{79 \times 79} \quad (3)$$

The eigenvalues of Eq. (3) is denoted by λ_i and the corresponding eigenvectors are $\psi_{E_i} = (c_{i1}, c_{i2}, \dots, c_{i79})^T$, where $i = 1, 2, \dots, 79$. Then, we can project our initial input wave packet ψ_{in} , e.g., taken $\psi_{in} = (0, \dots, 0, 1, 0, \dots, 0)_{79 \times 79}$ as single-site excitation, into all eigenstates ψ_{E_i} , and result in a series of occupation weight on each eigenstate as

$$\mathbf{p} = \Psi_{in} \cdot \Psi_E = (p_1, p_2, \dots, p_i, \dots, p_{78}, p_{79}). \quad (4)$$

Then it is easy to make a Fourier Transform of the field distribution with respect to the eigenvectors in their weight factors to determine the excitation intensity on k_x components in the dispersion spectrum as

$$\psi_{E_i}(k) = p_i \sum_n \psi_{E_i}(n) \exp(-ink), \quad (5)$$

where n is the lattice number. With the rigorous analytical solution of the coupled mode equation above, we can draw the dispersion spectrum of the PRWA under different excitation conditions. For simplicity, we fix coupling coefficients as 0.03 and -0.03 and ignore the loss. Figure 4(a)-4(c) plot the excited band structure under the excitation conditions of single-site, 3-sites and 7-sites, whose propagation results calculated by CMT are shown in Fig. 4(d)-4(f) correspondingly. Obviously, in despite of the same dispersion relation, different excitations result in different intensity weight on k_x spectrum, which gives rise to different propagation properties in such a coupled waveguide array system. As we can see, the 7-sites excitation produces a quite good 1D nondispersive conical diffraction in a splitting manner. It is because that with more excitation sites the excitation modes are more concentrated at the center of Brillouin zone with linear dispersions shown as Fig. 4(c). While for less-sites excitations (especially the single-site one), the whole range of the band will be excited because smaller excitation port corresponds to wider k_x bandwidth, and those nonlinear dispersion parts at the Brillouin boundary will make contributions (see Fig. 4(a) and 4(b)). Then it results in dispersive diffractions as the quantum walk profile in a periodic waveguide array [25,26], as shown in Fig. 4(d) and 4(e). In our case, selecting 7-sites as excitation is good enough to demonstrate the 1D conical diffraction as simulation for massless Dirac dynamics (see Fig. 3(d) and 4(f)). By a more careful investigation, it is found that the maximum peak intensity increases as the excitation waveguide from single-site to 7-sites one (all the intensities are normalized with input total energy as 1 unit). In the viewpoint of quantum walk property, this 1D nondispersive conical diffraction case corresponds to a faster walker with more field weight at the boundaries. Therefore, such kind of behavior suggests a possible application in accelerating the quantum searching algorithm [25, 26].

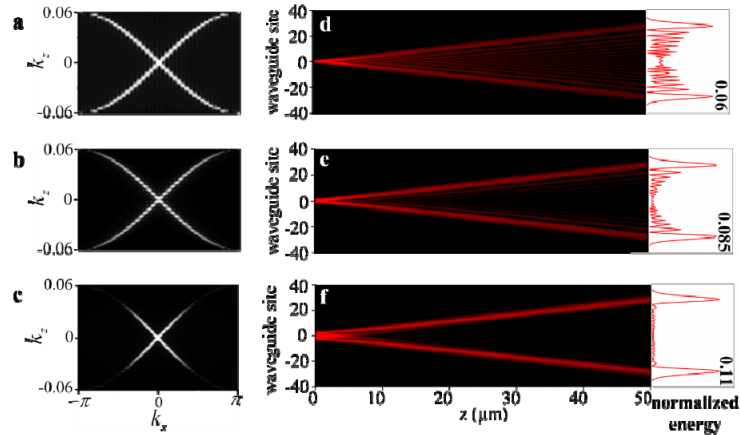


Fig. 4. Excited band structures of binary waveguide array with balanced coupling coefficients of -0.03 and 0.03 for (a) single-site excitation, (b) 3-sites excitation and (c) 7-sites excitation. (d-f) are the corresponding beam propagation patterns (left panel) and end-face intensity distributions (right panel) for (a-c).

3.2 Influence of loss on simulation results

Last but not the least, we consider the influence of loss on our massless Dirac simulation in a viewpoint of more practical case, and the COMSOL simulation with imaginary part of silver material ($\epsilon = -18.2947 + 0.4808i$ at $\lambda = 633$ nm according to Ref [27].) is shown as Fig. 5(b). As compared with lossless one (Fig. 5(a)), it is clearly found that the SPP propagations are almost in the same profile, though there are apparent energy dissipations in lossy system shown as Fig. 5(c). It surely confirms that such a plasmonic ridge waveguide array system is valid to simulate the behavior of massless Dirac dynamics, and suggests feasible experiments as the precise nano-structure sample being fabricated.

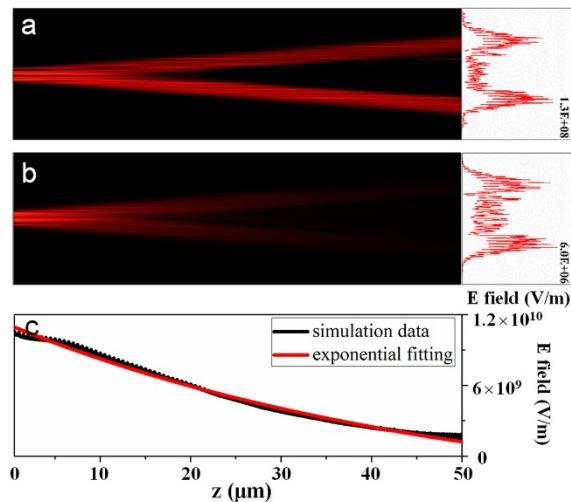


Fig. 5. Simulation results of (a) lossless system and (b) lossy system with output intensity distributions shown on the right. Here the propagation distance is $50 \mu\text{m}$ with 9 waveguide sites excited in both cases. (c) Summation of electric field intensity in all waveguides along propagating length in lossy system. The fitting curve shows an obvious exponential attenuation during propagation.

4. Conclusion

In conclusion, we studied the coupling property of SPP modes in a coupled ridge waveguide system, in which positive and negative couplings were mainly investigated and properly designed thanks to the vectorial nature SPP modes. Based on these analyses binary plasmonic waveguide arrays with alternating positive and negative coupling coefficients were theoretical modeled to simulate transporting behavior of massless Dirac dynamics. Both CMT calculation and full-wave simulation results show good evidence of the linear dispersion with two splitting nondispersive propagations that agree well with the characteristic of massless Dirac dynamics. We also discuss the influence of excitation condition on beam propagation via theoretical calculation based on coupled mode theory, and interpreted the importance of proper excitation condition. Lastly, the numerical result with loss-included plasmonic system indicates the possible realization in experiments. Our results reveal the strong flexibility in tailoring the coupling property as well as the dispersion engineering in waveguide array system, which would possibly provide a platform to simulate or mimic further interesting physics that is hardly achievable in other system.

Funding

National Key R&D Program of China (2017YFA0303700, 2016YFA0202103), National Natural Science Foundation of China (No. 11674167, 11621091).

Acknowledgment

T. Li thanks the supports of PAPD from Jiangsu Province and the Dengfeng Project B of Nanjing University.